

Numerical Studies of Quantum Hall Ferromagnetism in Two-Subband Systems

Xiao-Jie Hao⁽¹⁾, Tao Tu⁽¹⁾,* Yong-Jie Zhao⁽¹⁾, Guang-Can Guo⁽¹⁾, H. W. Jiang⁽²⁾, and Guo-Ping Guo^{(1)†}

⁽¹⁾ *Key Laboratory of Quantum Information, University of Science and Technology of China,
Chinese Academy of Sciences, Hefei 230026, People's Republic of China*

⁽²⁾ *Department of Physics and Astronomy, University of California at Los Angeles,
405 Hilgard Avenue, Los Angeles, CA 90095, USA*

(Dated: November 25, 2018)

We carry out a numerical study of the quantum Hall ferromagnetism in a two-subband system using a set of experimental parameters in a recently experiment [X. C. Zhang, I. Martin, and H. W. Jiang, Phys. Rev. B **74**, 073301 (2006)]. Employing the self-consistent local density approximation for growth direction wave function and the Hartree-Fock theory for the pseudospin anisotropy energy, we are able to account for the easy-axis and easy-plane quantum Hall ferromagnetism observed at total filling factor $\nu = 3$ and $\nu = 4$, respectively. Our study provides some insight of how the anisotropy energy, which highly depends upon the distribution of growth direction wave functions, determines the symmetry of the quantum Hall ferromagnets.

PACS numbers: 73.43.Nq, 71.30.+h, 72.20.My

I. INTRODUCTION

Multi-component quantum Hall systems have exhibited a collection of interesting phenomena which are the manifestation of electronic correlations [1]. Such correlations become particularly prominent when two or more sets of Landau levels (LLs) with different layer, subband, valley, spin, or Landau level indices are brought into degeneracy [2, 3, 4, 5]. In experimental systems, different LLs can be tuned to cross by varying gate voltage, charge density, magnetic field or the magnetic field tilted angle to the sample. One of the attractions is the formation of quantum Hall ferromagnets (QHF) due to the exchange interactions of the two subbands states, termed as pseudospins [6, 7]. Self-consistent local density approximation (SCLDA) and Hartree-Fock mean field method can be performed on the calculation of ground state energy and quasi-particle energy gap [4, 7, 8, 9].

Recent experiments in single quantum well with two-subband occupied systems [10, 11], showed evidence of QHF when two LLs were brought into degeneracy. The QHF can either be easy-axis or easy-plane, depending on the details of LL crossing configurations [10, 11]. In this paper we follow the theoretical framework of Jungwirth and MacDonald [8] and numerically calculate the pseudospin anisotropy energy using the sample parameters in the experiment of Zhang *et al.* [11]. The result confirms the QHF taking place at total filling factor $\nu = 3$ and $\nu = 4$ are expected to be easy-plane and easy-axis QHF, respectively. As we will discuss in this paper, the gate bias voltage, which affects the spatial distributions of the wave functions of the two subbands, plays a leading role in the formation of easy-plane and easy-axis QHF.

*Electronic address: tutao@ustc.edu.cn

†Electronic address: gpguo@ustc.edu.cn

II. PSEUDOSPIN QUANTUM HALL FERROMAGNETS

The pseudospin representation is used to describe the valence LLs degenerated in the Fermi level [7, 8]. Following the theoretic studies of pseudospin QHFs [7, 8], here we focus on a two-subband two dimensional electron system, in which the LLs are labeled by (ξ, n, s) , where $\xi = S/A$ is first/second subband (in the no biased quantum well, also called symmetry/antisymmetry subband) index, $n = 0, 1, \dots$ is Landau level in-plane orbit radius quantum number, and $s = \pm\frac{1}{2}$ represents real spin. When two LLs are brought close to degeneracy but still sufficiently far from other LLs, one of them can be labeled as pseudospin up ($\sigma = \uparrow$) and the other as pseudospin down ($\sigma = \downarrow$). In the experimental work of Zhang *et al.* [11], as shown in Fig. 1, we can label pseudospin up ($\sigma = \uparrow$) as $(S, 1, \frac{1}{2})$ and pseudospin down ($\sigma = \downarrow$) as $(A, 0, \frac{1}{2})$ at filling factor $\nu = 3$. At filling factor $\nu = 4$, we label pseudospin up ($\sigma = \uparrow$) as $(S, 1, \mp\frac{1}{2})$ and pseudospin down ($\sigma = \downarrow$) as $(A, 0, \pm\frac{1}{2})$. Here the upper and lower signs before spin index refer to the crossing point at lower and higher magnetic field, respectively.

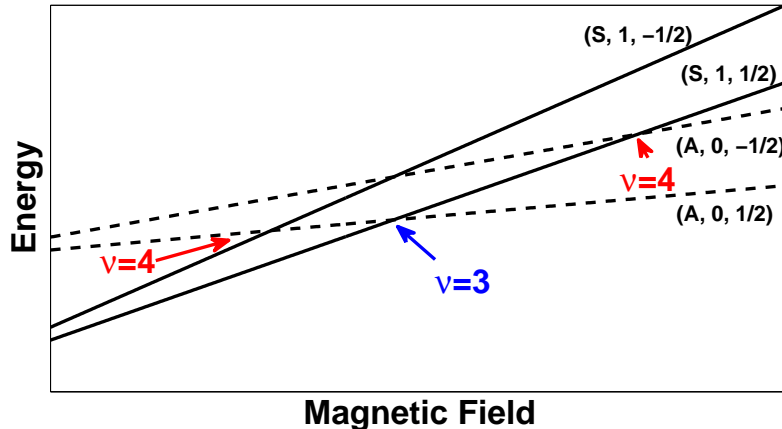


FIG. 1: Landau level diagram of two-subband system. Four Landau levels labeled by (ξ, n, s) are crossing to each other during the increasing of the magnetic field (see text for details). Three arrows point out the crossing point of Landau levels at filling factor $\nu = 3$ and $\nu = 4$.

At this moment, we would emphasize the essential similarity between two-subband system and ordinary bilayer system (double quantum well). On one hand, due to a separation of charges to opposite sides of the well originating from the Coulomb repulsion, a wide single quantum well can be modeled as an effective bilayer system [4, 8, 12]. Therefore in a single quantum well two-subband structure, the states of electrons can be characterized by two parameters similar to a bilayer system: the tunneling gap Δ_{SAS} and effective layer separation d . The Δ_{SAS} is chosen as equal to the difference between the lowest two subband energy levels and d is given by the distance between two centers of the charge distribution in this single quantum well. On the other hand, let us assume the two dimensional electron gas is in the $x - y$ plane in the following calculation and discussion, so the sample growth direction is aligned with the z axis. In a no biased bilayer system, although the layer wave function in z direction is spatially separated in two layers, once included in the effect of tunneling between two layers Δ_t and rediagonalized the z direction Hamiltonian, it will be just

like the two-subband system which has symmetry and antisymmetry subbands. And the symmetry-antisymmetry gap Δ_{SAS} is equal to the inter-layer tunneling Δ_t . Even when a bias voltage between two layers exists, the circumstance is more or less the same. Since they are theoretically identical, all the pseudospin language theory used in bilayer system is available in the two-subband system.

While pseudospin up and pseudospin down LLs are degenerate but the number of electrons is not enough to fill all the two LLs, electrons will stay in a broken-symmetry ground state. Actually, the state electrons choosing is a linear combination of two pseudospin LLs which minimizes the system total energy. Typically, the many-body ground state can be written as follows [8]:

$$|\Psi[\hat{m}]\rangle = \prod_{k=1}^{N_\phi} c_{\hat{m},k}^\dagger |0\rangle, \quad (1)$$

where $c_{\hat{m},k}^\dagger$ creates the single-particle state oriented in a certain unit vector $\hat{m} = (\sin\theta \cos\varphi, \sin\theta \sin\varphi, \cos\theta)$ with wave function:

$$\psi_{\hat{m},k}(\vec{r}) = \cos\left(\frac{\theta}{2}\right)\psi_{\uparrow,k}(\vec{r}) + \sin\left(\frac{\theta}{2}\right)e^{i\varphi}\psi_{\downarrow,k}(\vec{r}). \quad (2)$$

Here $\psi_{\sigma,k}(\vec{r})$ is the single-particle state wave function which contains growth direction subband wave function $\lambda_\xi(z)$ and in-plane LL wave function $L_{n,s,k}(x,y)$:

$$\psi_{\sigma,k}(\vec{r}) = \lambda_\xi(z)L_{n,s,k}(x,y). \quad (3)$$

Then the Hartree-Fock energy of the system can be obtained as following [8]:

$$E_{HF}(\hat{m}) \equiv \frac{\langle\Psi[\hat{m}]|H|\Psi[\hat{m}]\rangle}{N_\phi} = - \sum_{i=x,y,z} \left(E_i - \frac{1}{2}U_{1,i} - \frac{1}{2}U_{i,1} \right) m_i + \frac{1}{2} \sum_{i,j=x,y,z} U_{i,j} m_i m_j. \quad (4)$$

Whether the ground state is easy-axis or easy-plane only depends on the quadratic coefficient in pseudospin magnetization m_i (i.e. the pseudospin anisotropy energy U_{xx} , U_{yy} and U_{zz}):

$$U_{ij} = \frac{1}{4} \int \frac{d^2\vec{q}}{(2\pi)^2} v_{ij}(0) - \frac{1}{4} \int \frac{d^2\vec{q}}{(2\pi)^2} v_{ij}(\vec{q}). \quad (5)$$

The first $\vec{q}=0$ term in Eq. (5) is the Hartree term and the second term is the Fock term. $v_{ij}(\vec{q})$ can be expanded to sum of several pseudospin matrix elements $v_{\sigma'_1, \sigma'_2, \sigma_1, \sigma_2}(\vec{q})$, which are products of subband and the in-plane parts [8]. If $U_{zz} < U_{xx} = U_{yy}$, the system is in easy-axis QHF, which means the pseudospin magnetization \hat{m} is aligned either up or down; and if $U_{zz} > U_{xx} = U_{yy}$, the system is in easy-plane QHF, which is a coherent superposition of the two pseudospin LLs.

III. GROWTH DIRECTION WAVE FUNCTION CALCULATION USING SCLDA

We numerically calculate the growth direction (z direction) wave function $\lambda_\xi(z)$ in Eq. (3) using SCLDA to compare the pseudospin anisotropy energy U_{xx} and U_{zz} in Eq. (4) [13]. In the SCLDA method, wave function $\lambda(z)$ is described

by the Schrödinger equation:

$$\left(-\frac{1}{2m^*} \frac{\partial^2}{\partial z^2} + V_b(z) + V_{gate}(z) + V_{xc}(z) + V_H(z)\right) \lambda_i(z) = \varepsilon_i \lambda_i(z). \quad (6)$$

Here m^* is the effective electron mass in GaAs, V_b corresponds to the conduction band discontinuity, V_{gate} is the bias potential caused by the difference of front and back gate voltage $|\Delta V_g|$, V_{xc} refers to the exchange-correlation potential related to the electron charge distribution $n(z)$ (We use the form of V_{xc} given by Hedin and Lundqvist [14]). The Hartree term V_H due to electrostatic potential is given in the Poisson equation:

$$V_H(z) = -\frac{2\pi e^2}{\epsilon} \int dz' |z - z'| n(z'). \quad (7)$$

The subband energies ε_ξ , wave functions $\lambda_\xi(z)$ and the electron charge distributions $n_\xi(z)$ of both subbands can be calculated by solving the Schrödinger equation Eq. (6) and the Poisson equation Eq. (7) simultaneously [15].

IV. NUMERICAL RESULT AND DISCUSSION

Taking the unit of energy as $e^2/\epsilon l_B$ (l_B is the magnetic length), we calculate the pseudospin anisotropy energy U_{xx} , U_{yy} and U_{zz} at filling factor $\nu = 3$ and $\nu = 4$ in Zhang *et al.*'s work [11]. At total filling factor $\nu = 3$, $U_{xx} \equiv U_{yy} = -0.370 < U_{zz} = 0.017$, so the system will stay in easy-plane QHF. At one degenerate point of total filling factor $\nu = 4$, $U_{xx} \equiv U_{yy} = 0 > U_{zz} = -0.1266$, and at the other degenerate point $U_{xx} \equiv U_{yy} = 0 > U_{zz} = -0.1293$. Both of the energy differences of $U_{zz} - U_{xx}$ at $\nu = 4$ indicate easy-axis QHF ground states.

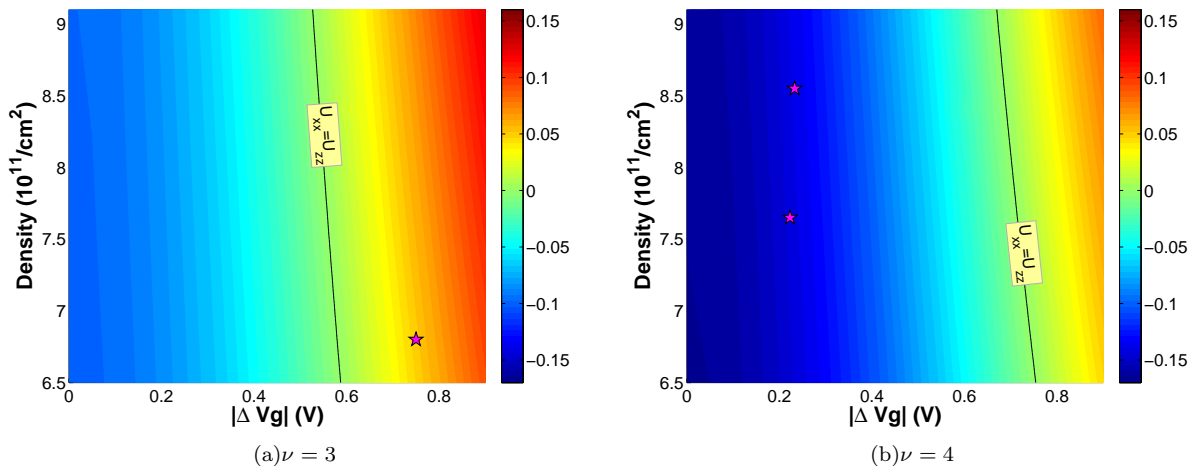


FIG. 2: (Color online) Phase diagram of $U_{zz} - U_{xx}$ (unit: $e^2/\epsilon l_0$) at filling factor (a) $\nu = 3$ and (b) $\nu = 4$. In the $U_{zz} - U_{xx} < 0$ (left/blue) region easy-axis QHF is energetically favorable while in the $U_{zz} - U_{xx} > 0$ (right/red) region, easy-plane QHF is favorable. Black lines in each figure labeled by $U_{xx} = U_{zz}$ show the critical positions where a quantum phase transition from easy-axis to easy-plane QHF occurs. The three stars in these two figures denote the $\nu = 3$ and $\nu = 4$ experimental parameter in the experimental work of Zhang *et al.*.

To illustrate the evolution from easy-axis QHF to easy-plane QHF, we calculate the phase diagrams of $U_{zz} - U_{xx}$ as a function of bias gate voltage $|\Delta V_g|$ and total density n at filling factor $\nu = 3$ (Fig. 2(a)) and $\nu = 4$ (Fig. 2(b)).

In the following discussion, in order to make consistency, we choose $e^2/\epsilon l_0$ ($l_0 = 10nm$) as the unit of energy. In the phase diagram (Fig. 2), we label the density and bias voltage $|\Delta Vg|$ position where the crossing occurs in the experimental work of Zhang *et al.* [11]. In the left/blue (right/red) parts of each figure (Fig. 2(a) and Fig. 2(b)), where $U_{zz} < (>)U_{xx}$, easy-axis (easy-plane) has the lower electron interaction energy. From Fig. 2, we find that the anisotropy energy difference $U_{zz} - U_{xx}$ is very sensitive to the bias voltage $|\Delta Vg|$. If we could vary the gate voltage across the black line labeled $U_{xx} = U_{zz}$ from left to right in a determined density, a quantum phase transition from easy-axis to easy-plane QHF will happen.

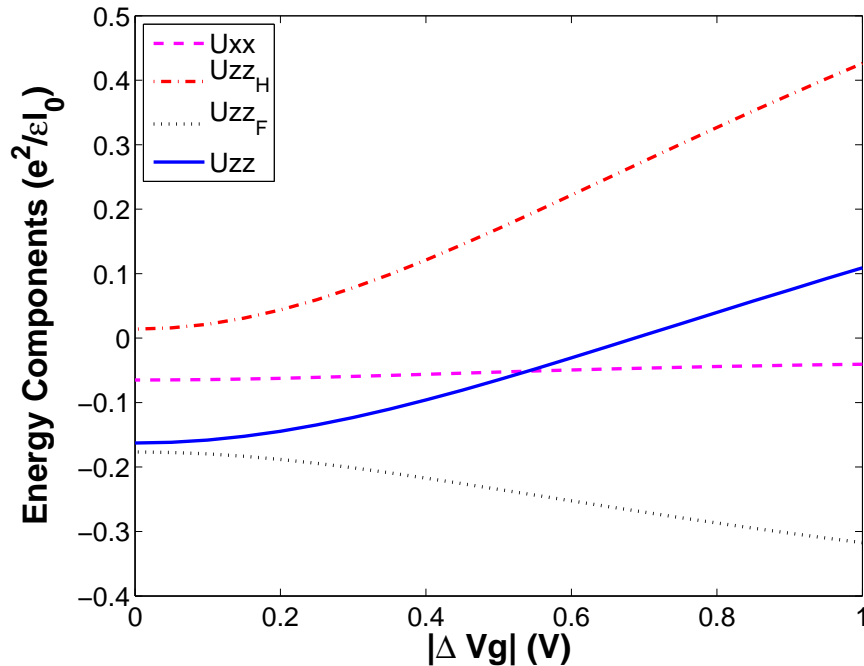


FIG. 3: Energy components of anisotropy energy U_{xx} and U_{zz} v.s. bias voltage $|\Delta Vg|$. Except for $U_{xx} \equiv 0$ at $\nu = 4$, all the other terms are same at filling factor $\nu = 3$ and $\nu = 4$. U_{zzH} and U_{zzF} correspond to the Hartree term and Fock term in the Hartree-Fock calculation of U_{zz} .

In order to make a comparison of the effect of each term in anisotropy energy, we plot them in Eq. (5) as a function of $|\Delta Vg|$ at a certain density of $8.5 \times 10^{11}/cm^2$ in Fig. 3. Here we have to point out that all the formulas at $\nu = 3$ and 4 are the same, except that U_{xx} vanishes at $\nu = 4$. So the Fig. 3 is applicable to both filling factor $\nu = 3$ and $\nu = 4$ only if in the $\nu = 4$ situation the U_{xx} term is set to a constant zero. The reason for the different behavior of U_{xx} at filling factor $\nu = 3$ and $\nu = 4$ will be discussed in the following. Note that the dominated term in $U_{zz} - U_{xx}$ is the Hartree term U_{zzH} , which is due to the electrostatic potential of electrons. It shows that the U_{zzH} term increases immediately with the increasing bias voltage $|\Delta Vg|$.

To examine what the role the bias voltage plays in the determination of easy-plane or easy-axis QHF, we give some SCLDA results in the Fig. 4. We define an effective subband separation Δd to describe the distance between the cores of first and second subbands wave functions. The $|\Delta d|$ as a function of bias voltage is plotted in Fig. 4, also with some

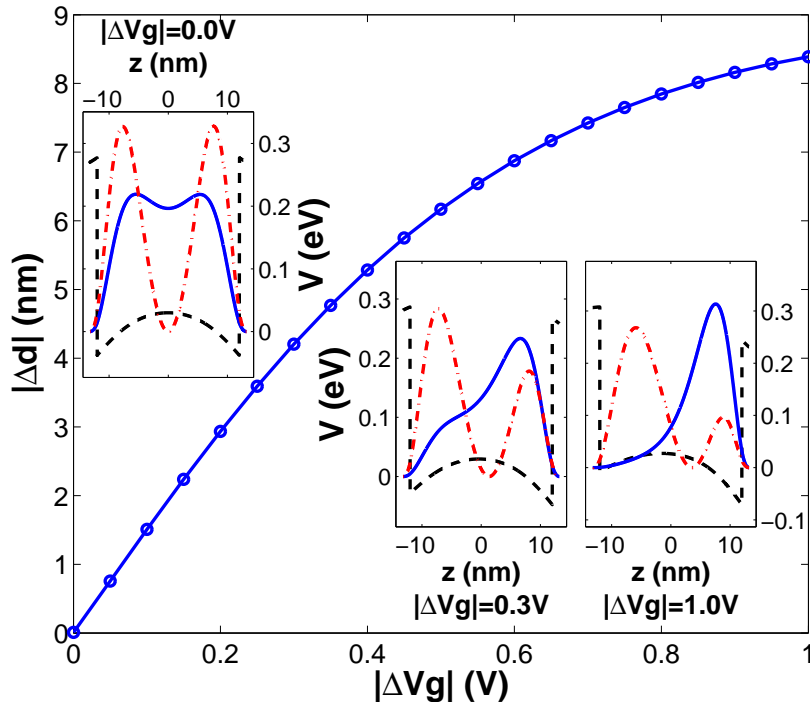


FIG. 4: (Color online) Effective subband separation $|\Delta d|$ as a function of bias gate voltage $|\Delta V_g|$ at the density of $8.5 \times 10^{11}/\text{cm}^2$. Three insets show the well profiles (black dashed lines) with first (blue solid lines) and second (red dash-dot lines) subbands wave functions at different bias voltage: $|\Delta V_g| = 0.0V$, $0.3V$, and $1.0V$.

demonstrations of quantum well configurations and subbands wave functions in different bias voltages ($|\Delta V_g| = 0.0V$, $0.3V$, and $1.0V$). The data in Fig. 4 are all selected from the same density $8.5 \times 10^{11}/\text{cm}^2$ as in Fig. 3. It is obvious that the bias gate voltage changes the effective separation of two subbands while changing the well potential $V_{gate}(z)$ in Eq. (6). The larger the bias voltage is added, the farther the lowest two subbands are separated. Since at a well separated z direction wave function configuration, all the electrons near the Fermi level filling in the same subband, i.e. the same pseudospin level, will raise a larger electrostatic energy, the easy-axis QHF is not favorable. Thus an easy-plane QHF can save more Hartree energy in the larger bias voltage situation. On the other hand, when the potential of the quantum well maintains a good symmetry in the small bias voltage limit, electrons can pick up one of the two pseudospin levels to keep the Hartree energy minimal and avoid the energetic penalty from inter-subband tunneling as well.

As mentioned before, the difference of U_{xx} between total filling factor $\nu = 3$ and $\nu = 4$ could be explained in the similar way. The anisotropy energy U_{xx} or U_{yy} is constituted of Hartree part and Fock part (see Eq. (5)). In our numerical calculation, we find that the Hartree terms of U_{xx} and U_{yy} are always zero at both $\nu = 3$ and $\nu = 4$. And the only non-zero term in U_{xx} or U_{yy} is the Fock term $U_{xxF} \equiv U_{yyF} < 0$ at filling factor $\nu = 3$, which owes to the exchange interaction. It implies that at filling factor $\nu = 4$, where pseudospin up $\sigma = \uparrow (S, 1, \mp \frac{1}{2})$ and pseudospin down $\sigma = \downarrow (A, 0, \pm \frac{1}{2})$ have opposite real spins, the easy-plane anisotropy, in which the electrons stay in both subband

equally, would cost much more exchange energy. But at $\nu = 3$ the pseudospin up $\sigma = \uparrow (S, 1, \frac{1}{2})$ and pseudospin down $\sigma = \downarrow (A, 0, \frac{1}{2})$ have the same spin. Then there is no such problem need to be considered. Therefore, the easy-axis QHF is more likely to happen at total filling factor $\nu = 4$ than $\nu = 3$.

On the basis of above discussion, we may summarize as following. The bias gate voltage added to the sample changes the quantum well profile in the growth direction as well as the spacial separation of the lowest two subbands wave functions. For a larger bias gate voltage, the potential of the well is much skewer, so the two subbands wave functions locate in the opposite side of the quantum well (inset of Fig. 4). As a result, the Hartree energy will arise if all the electrons stay in one narrow subband or pseudospin level. Thus a easy-plane QHF, in which the electrons fill the two pseudospin levels equally, is more energetically favorable at a large bias gate voltage. In addition, a state with opposite real spins will expend more exchange energy, so the easy-plane QHF is more easily to form at a pseudospin configuration in which the two pseudospin level have the same real spin (filling factor $\nu = 3$ in this paper).

V. CONCLUSION

Using self-consistent local density approximation method and Hartree-Fock mean field theory, we calculated wave function in the growth direction and the anisotropy energy in the two-subband quantum Hall system. The data shows great consistent with the observed easy-plane and easy-axis quantum hall ferromagnets at filling factor $\nu = 3$ and $\nu = 4$ in the experiment of Zhang *et al.* [11]. Also, by analyzing the numerical result, we give an easy-to-understand explanation about the anisotropy occurring at these filling factors.

Acknowledgments

This work was funded by National Fundamental Research Program, the Innovation funds from Chinese Academy of Sciences, NCET-04-0587, and National Natural Science Foundation of China (Grant No. 60121503, 10574126, 10604052).

-
- [1] R. E. Prange and S. M. Girvin (eds.), *The Quantum Hall Effect* 2nd edn (Springer, New York, 1990).
 - [2] S. Q. Murphy, J. P. Eisenstein, G. S. Boebinger, L. N. Pfeiffer, and K. W. West, Phys. Rev. Lett. **72**, 728 (1994).
 - [3] K. Yang, K. Moon, L. Zheng, A. H. MacDonald, S. M. Girvin, D. Yoshioka, and S. C. Zhang, Phys. Rev. Lett. **72**, 732 (1994).
 - [4] V. Piazza, V. Pellegrini, F. Beltram, W. Wegscheider, T. Jungwirth, and A. H. MacDonald, Nature **402**, 638 (1999).
 - [5] Y. P. Shkolnikov, E. P. De Poortere, E. Tutuc, and M. Shayegan, Phys. Rev. Lett. **89**, 226805 (2002).
 - [6] For a review on quantum Hall ferromagnets, see experimental chapter by J.P. Eisenstein and theoretical chapter by S. M. Girvin and A. H. MacDonald in S. Das Sarma and A. Pinczuk (eds.), *Perspectives on Quantum Hall Effects* (Wiley, New York, 1997).
 - [7] A. H. MacDonald, P. M. Platzman, and G. S. Boebinger, Phys. Rev. Lett. **65**, 775 (1990).
 - [8] T. Jungwirth and A. H. MacDonald, Phys. Rev. B **63**, 035305 (2000).
 - [9] T. Jungwirth, S. P. Shukla, L. Smrčka, M. Shayegan, and A. H. MacDonald, Phys. Rev. Lett. **81**, 2328 (1998).
 - [10] K. Muraki, T. Saku, and Y. Hirayama, Phys. Rev. Lett. **87**, 196801 (2001).
 - [11] X. C. Zhang, I. Martin, and H. W. Jiang, Phys. Rev. B **74**, 073301 (2006).
 - [12] M. Abolfath, L. Belkhir, and N. Nafari, Phys. Rev. B **55**, 10643 (1997).

- [13] F. Stern and S. Das Sarma, Phys. Rev. B **30**, 840 (1984).
- [14] L. Hedin and B. I. Lundqvist, J. Phys. C **4**, 2064 (1971).
- [15] J. M. Blatt, J. Comp. Phys. **1**, 382 (1967).